Positron Injection and Acceleration on the Wake Driven by an Electron Beam in a Foil-and-Gas Plasma

X. Wang,[1] R. Ischebeck,[2] P. Muggli,[1] T. Katsouleas,[1] C. Joshi,[3] W. B. Mori,[3] and M. J. Hogan[2]
[1]*University of Southern California, Los Angeles, California 90089, USA*
[2]*Stanford Linear Accelerator Center, Stanford, California 94025, USA*
[3]*University of California at Los Angeles, Los Angeles, California 90095, USA*
(Received 11 March 2008; published 17 September 2008)

A novel approach for generating and accelerating positron bunches in a plasma wake is proposed and modeled. The system consists of a plasma with an embedded thin foil into which two electron beams are shot. The first beam creates a region for accelerating and focusing positrons and the second beam provides positrons to be accelerated. Monte Carlo and 3D PIC simulations show a large number of positrons ($10^7 \sim 10^8$) are trapped and accelerated to ~5 GeV over 1 m with relatively narrow energy spread and low emittance.

DOI: 10.1103/PhysRevLett.101.124801 PACS numbers: 41.75.Ht, 41.75.Lx, 52.40.Mj

Recently, a plasma wakefield accelerator (PWFA) experiment at the Stanford Linear Accelerator Center (SLAC) has demonstrated that electrons can be accelerated by up to 43 GeV in a 85 cm long plasma [1]. PWFA is a promising approach for reducing the size and cost of a future electron or positron (e^- or e^+) linear collider [2]. To realize an (e^- or e^+) collider, ultrahigh gradient acceleration of positrons is equally important to that of electrons. However, acceleration of high-quality positron beams in plasmas is more challenging [3], and has been less studied experimentally due to the lack of suitable relativistic positron beams. Although focusing and acceleration of positron beams in plasmas have been demonstrated in proof-of-principle experiments, the acceleration has been in the linear regime with a modest acceleration gradient.

In the most recent PWFA experiments, electrons have been accelerated in the nonlinear wakes [4–6]. Such nonlinear wakes are excited when the force of a particle or a laser beam completely expels plasma electrons radially from the beam (Fig. 1). Acceleration of electrons in this nonlinear regime, so-called blowout [4] or bubble [5,6] regime, offers two striking advantages over the linear regime: a radially linear focusing field, and a large and radially independent accelerating field in the bubble. However, a nonlinear wake driven by a positron beam is fundamentally different from that driven by an electron beam, because plasma electrons are being pulled towards the axis rather than expelled from it. The plasma electrons starting at different radii do not reach the axis at the same time, and phase mix within the first oscillation. As a result, the accelerating field of a positron driver is found to be 2 to 5 times smaller than an electron driver with similar parameters [7,8]. Also, the focusing field inside the positron bunch is nonuniform axially and radially, which can result in emittance growth of the accelerated bunch [9]. It is therefore attractive to explore the acceleration of a tightly focused short positron bunch on the wake driven by an electron bunch [10] (or alternatively a laser pulse). Positrons can be accelerated and focused in a small volume of the wake located right behind the blowout bubble where the plasma electrons return to the axis to form a density compression (Fig. 1).

Experimentally, the simultaneous transport of very closely spaced electron and positron bunches (i.e., much less than a rf wavelength) in the same beam path is problematic in conventional rf accelerators. There are no current facilities capable of providing a positron bunch that follows an electron bunch by a few hundred microns. In this Letter, we present a new approach that overcomes these obstacles to generate and place positrons on the plasma wake of an electron bunch.

The idea is illustrated in Fig. 2 and described as follows: Two closely spaced in time electron bunches are focused on a thin foil target of high-Z material, such as Tantalum, placed at the entrance of a plasma. Positrons are produced through pair creation by the energetic bremsstrahlung photons generated by the electron beams in the foil target. Four bunches emerge from the foil target—two newborn positron bunches (of lesser current than the original electron bunches) superimposed with the two original electron bunches (note that two additional newborn electron bunches are born with lesser current than the original

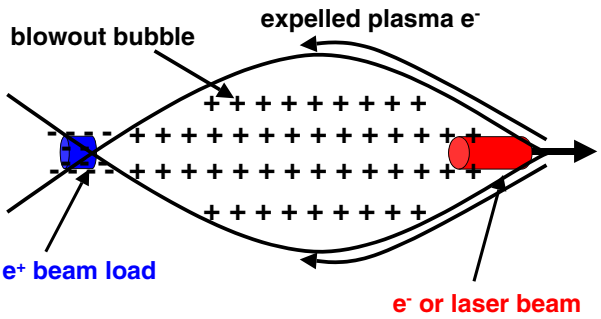

FIG. 1 (color online). Schematic of positron acceleration in the wake driven by an electron or laser beam driver.

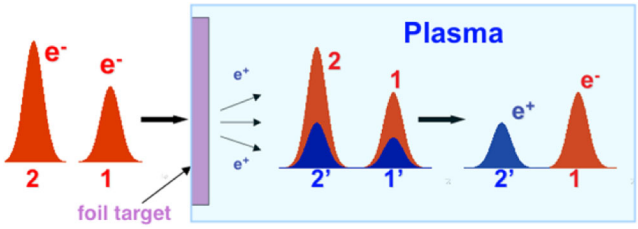

FIG. 2 (color online). Schematic positron generation and loading scheme. The two incoming electron bunches (1, 2) generate two positron bunches (1′, 2′) in a thin foil target. Only the drive electron bunch (1) and positron beam load (2′) remain in the plasma after a short distance.

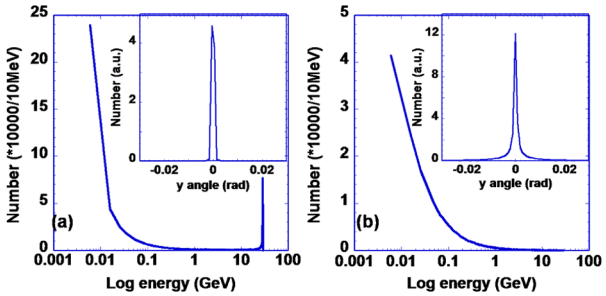

FIG. 3 (color online). EGS5 simulation results after a 0.5 mm Tantalum target: energy spectra of (a) the electron bunch and of (b) the produced positron bunch. Insets are the angular distributions in the y direction.

electron bunches and therefore are insignificant). The foil thickness is chosen such that the first electron bunch is only mildly scattered, and is still able to excite a large amplitude plasma wake after the foil. Either the spacing between the two electron bunches or the plasma density is adjusted such that the second bunch lies right behind the blowout bubble created by the first bunch (Fig. 1). The strong radial fields of plasma wake defocus the second electron bunch but focus the second positron bunch. The situation is reversed in the bubble: the strong radial fields focus the first electron bunch but defocus the first positron bunch. Thus after a short distance in the plasma, only the first electron bunch and second positron bunch, or positron beam load, remain, and the desired configuration of Fig. 1 is obtained. In the remainder of this Letter, we first model collision of the electron bunches with the foil target to obtain the phase space of the emerging electron and positron bunches. We then model self-consistently the propagation of these bunches in a plasma using a particle-in-cell (PIC) code. Finally, we discuss examples for beam parameters feasible at SLAC, and explore optimizing the beam quality of the positron beam load by varying the charge of the trailing (second) electron bunch.

To model positron generation in the foil target we use the Monte-Carlo code EGS5 [11]. The code includes energy loss of particles through ionization, bremsstrahlung radiation, pair production, etc. It can model the full phase space of the primary electrons and the secondary positrons after the foil target. Typical EGS5 simulations of a 0.5 mm Tantalum target show that the 28.5 GeV primary electron beam suffers relatively small energy loss in the target [Fig. 3(a)], and that the positron yield is about 5%. The secondary positrons have an approximately exponential energy distribution [Fig. 3(b)]. Most of the positrons are born with relativistic forward energy suitable for injecting into the plasma wake. The angular (Fig. 3) and spatial distributions of the secondary positrons follow those of the primary electrons. The spot sizes of the secondary positron bunches and the electron bunches are approximately the same, which are 2.5 μm in the x direction and 0.8 μm in the y direction; and the r.m.s angles of the positron bunches and the electron bunches are similar. The normalized emittances of the electron bunches before the foil target are 100 mm mrad in the x and 10 mm mrad in the y direction, and the geometric emittances are 0.001 78 and 0.000 18 mm mrad, respectively. After the foil target, the geometric emittances of the electron bunches become 0.001 88 and 0.000 23 mm mrad, and those of the newly generated positron bunches are 0.002 18 and 0.000 31 mm mrad [12]. EGS5 simulations for a Tantalum target with a thickness from 0.5 to 2 mm demonstrate that the positron yield is from 5% to 65%, and that the corresponding emittance growth of the primary electron bunch is 3% to 24%. EGS5 simulations also reveal that for a 1 mm Tantalum target the positron yield is only weakly dependent on the incoming electron beam energy, increasing from 17% to 26% for energies from 28 to 500 GeV.

Next we model plasma and beam dynamics resulting from the propagation of the four bunches downstream from the foil target using the three dimensional version of OSIRIS [13]. The size of the simulation window (x-y-z) is 71 μm $\times$ 71 μm $\times$ 360 μm and the number of grid points is 60 $\times$ 60 $\times$ 300, respectively. The simulation window moves at the speed of light, which is close to the beam velocity in the z direction. There are four particles per cell for the plasma and 1×10^6 super particles for each particle bunch. The time step for advancing particles and electromagnetic fields is $0.04\omega_p^{-1}$ (where ω_p is the plasma oscillation frequency) corresponding to an advancement of 0.95 μm for plasma density of 5×10^{16} cm^{-3}.

Simulations are performed for two cases with different amounts of charge in the trailing bunches, which correspond to light and heavy beam loading of the wake. The parameters are chosen to be feasible at SLAC [14] but with lower charge and lower plasma density. In both cases, the drive bunches have a bunch length of 7.4 μm, and there are 1.9×10^9 electrons in the electron driver and 8×10^7 positrons in the positron driver. The trailing bunches have a bunch length of 1.9 μm. The plasma density is 5×10^{16} cm^{-3}. In case 1, the electron trailing bunch has 5.0×10^8 electrons and the resulting positron trailing bunch has 2.0×10^7 positrons, the spacing between the drive and trailing bunches is 130 μm. In case 2, we attempt to optimize the positron beam load quality (injected charge,

relative energy spread, normalized emittance). To compensate for the low positron yield in the foil target, the number of electrons in the trailing bunch is increased to 1.4×10^{10}, and the resulting beam load has 5.6×10^{8} positrons. The optimal spacing between the drive and trailing bunches becomes 135 μm in this case.

Figure 4 shows the longitudinal and transverse wakefields from Case 1 simulation. In the lineout of the longitudinal wakefield [Fig. 4(a)], the positive peak accelerating field for positrons is about 7 GV/m, which is approximately twice that driven by a positron beam with similar parameters. The positrons are loaded around the peak-accelerating field. The positron beam loading in this modestly nonlinear regime is different from that in the nonlinear regime investigated by Lotov [10], in which externally injected positrons are loaded after the peak-accelerating field. Figure 4(b) shows that the accelerating field for positrons is not radially constant, which can introduce a relatively large final energy spread. Figure 4(c) shows that the focusing region for electrons is larger than that for positrons. This asymmetry worsens for positrons as the plasma wake becomes more nonlinear. For this reason, we have chosen somewhat smaller charge for the electron bunch than currently available. A region for both accelerating and focusing positrons is indicated by a vertical rectangle over Figs. 4(a) and 4(c). Figure 4(d) shows that the focusing field is not perfectly linear along the beam radius, which can lead to emittance growth of the accelerated positron bunch over the plasma length. Figure 5 shows the plasma, the electron beam and positron beam densities at early (left-hand) and late times (right-hand). In the left-hand panel ($s = 0.02$ cm), the two electron [Fig. 5(b)] and the two positron bunches [Fig. 5(c)] are still present. Further into the plasma ($s = 9.5$ cm), the plasma electron blowout is complete [Fig. 5(a′)], and the trailing electron bunch [Fig. 5(b′)] and the drive positron bunch [Fig. 5(c′)] have been defocused by the transverse wakefields and left the simulation box. Thus, the plasma functions as an efficient beam selector and the desired accelerating structure for positron beam load shown in Fig. 1 is established.

Figure 6(a) shows the energy at the peak of distribution and relative energy spread of the positron beam load along the plasma for the two cases. In both cases, the peak's energy increases linearly with the propagation distance as expected, while the relative energy spread asymptotically decreases. For Case 1, the beam load with 1.2×10^{7} positrons (in the energy range of $\pm$3FWHM about the

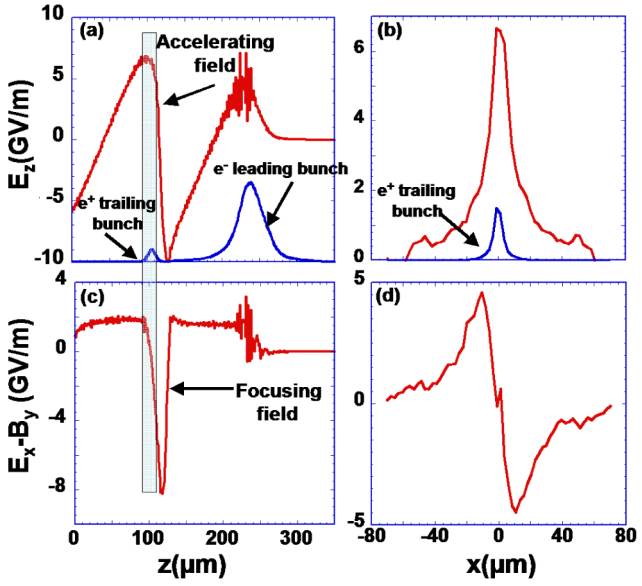

FIG. 4 (color online). 3D OSIRIS simulation results of plasma wakefields for case 1 at a distance 9.5 cm into the plasma: (a) longitudinal wakefield (E_z) lineout along the z axis, and (b) along x at $z = 107$ μm where the positron beam load is located; (c) transverse wakefield (E_x-B_y) lineout in the x-z plane along z at $x = 4.6$ μm; and (d) along x at $z = 107$ μm. In (a), the leading electron and the trailing positron bunch current profiles along z are indicated by the blue lines. The rectangle indicates the location where the wakefields are both accelerating and focusing for positrons and where the positron beam load is placed. In (c), the trailing positron bunch current profile along x is indicated by the blue line. Those bunches propagate to the right.

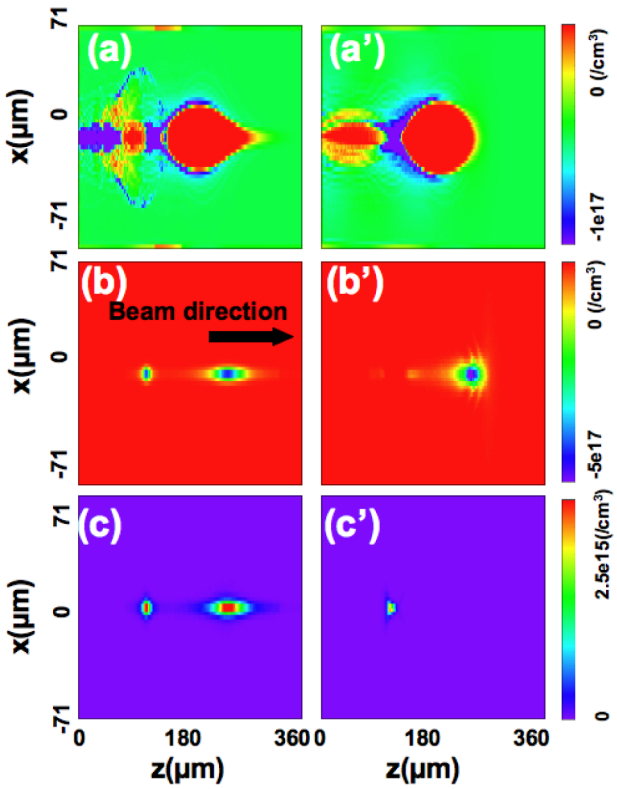

FIG. 5 (color online). 3D simulation results for case 1 after a propagation distance in the plasma of 0.02 cm (left-hand panels) and 9.5 cm (right-hand panels). x-z slices of the plasma density (a) and (a'), and electron beam density (b) and (b') and positron beam density (c) and (c'). [Note that maximum density is 1×10^{18} in (b) and 5×10^{17} in (b')].

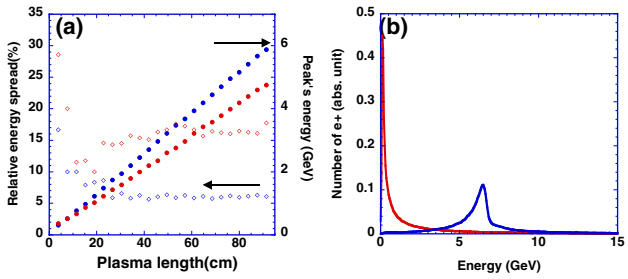

FIG. 6 (color online). (a) Evolution of the energy at the peak of distribution of the positron beam load for case 1 (blue solid circle) and case 2 (red solid circle), and the corresponding relative energy spread (blue and red hollow diamonds, respectively). (b) Energy spectra of the positron beam load after $s = 0.02$ cm (red line) and $s = 1$ m of plasma (blue line) for case 1.

peak's energy) reaches a peak's energy at 6.2 GeV with relative energy spread (quoted as FWHM/[(peak energy)/2]) of 6% after 1-m plasma. The normalized emittances of the positron bunch (quoted as r.m.s. momentum multiplied by r.m.s. spot size) are 20 mm mrad in the x and 25 mm mrad in the y direction, which are much lower than those of the incoming electron bunch. The bunch length of the positron beam load is about 6 μm, and the transverse spot sizes are about 2 μm in the x and 2.4 μm in the y direction. Figure 6(b) shows the beam load energy distribution after 0.02 cm and 1 m of plasma. In this example, 60% of positrons produced in the foil target are in the energy range of $\pm$3FWHM about the peak's energy after 1-m plasma. For case 2, 7.0×10^7 positrons or 13% of positrons produced in the foil target are injected in the energy range of $\pm$3FWHM about the peak's energy after 1-m plasma. Most of the positron loss occurs while the high current electron beam load is leaving the accelerating structure. This temporarily changes the wake loading and shifts the location for optimal positron beam loading. Once the high charge electron beam load is gone, the accelerating structure becomes stationary and the injected positrons remain trapped thereafter. The positron beam load is accelerated to 4.8 GeV with 16% relative energy spread after 1-m plasma, and the normalized emittances are 40 mm mrad in the x and y directions. The acceleration gradient is about 23% lower than in case 1 because of the higher charge positron beam loading on the plasma wake.

The scheme presented here provides a promising approach for accelerating positrons in the wake of an electron beam. It represents an opportunity to experimentally study the acceleration of positrons on an electron wake. For near-term experiments, the greatest technical challenge is to produce the initial two electron bunches; however, this is similar to the two-bunch electron wakefield acceleration experiment and is actively being pursued [15]. To extend this scenario to a high-energy collider requires increasing the number of particles and reducing the energy spread and the emittance of the positron beam load to increase the luminosity. There are several options for increasing the luminosity. One is to employ a high repetition rate accelerator while keeping the bunch charge relatively modest as in the examples in this Letter. Alternatively, one can increase the charge per bunch, but that can lead to a more nonlinear wake and ultimately requires a very short and narrow beam load with little tolerance for phase slippage or hosing. In order to increase the beam load charge, we can lengthen the drive bunch and lower the plasma density to remain in the modestly nonlinear regime by somewhat sacrificing the acceleration gradient. This also improves the opportunities for using beam loading to flatten the wakes and reduce the energy spread [16]. The tradeoffs and optimization of these choices will be the subject of future work.

This work supported by Department of Energy Contracts No. DE-FC02-01ER41192, No. DE-AC02-76SF00515 (SLAC), No. DE-FG03- 92ER40745, No. DE-FG52-06NA26195, No. DE-FG0392ER40727, No. DE-AC-0376SF0098, DE-FG02-03ER54721 and National Science Foundation Grants No. ECS-9632735, No. DMS-9722121, and No. PHY-0078715. Simulations were done at the USC Center for High Performance Computing and Communications (HPCC). Useful discussions with the members of the E-167 collaboration at SLAC are greatly acknowledged.

[1] I. Blumenfeld *et al.*, Nature (London) **445**, 741 (2007).
[2] S. Lee *et al.*, Phys. Rev. ST Accel. Beams **5**, 011001 (2002).
[3] C. Joshi *et al.*, Phys. Plasmas **9**, 1845 (2002).
[4] J. B. Rosenzweig *et al.*, Phys. Rev. A **44**, R6189 (1991).
[5] A. Pukhov and J. Meyer-ter-Vehn, Appl. Phys. B **74**, 355 (2002).
[6] W. Lu *et al.*, Phys. Rev. Lett. **96**, 165002 (2006).
[7] S. Lee *et al.*, Phys. Rev. E **64**, 045501 (2001).
[8] D. Bruthwiler *et al.*, *Proceedings of the 2003 Particle Accelerator Conference* (IEEE, Piscataway, NJ, 2003), p. 734.
[9] P. Muggli *et al.*, Phys. Rev. Lett. **101**, 055001 (2008).
[10] K. V. Lotov, Phys. Plasmas **14**, 023101 (2007).
[11] H. Hirayama *et al.*, The EGS Code System, SLAC-R-730 (2005).
[12] Geometric emmittance is calculated as r.m.s spot size multiplied by r.m.s. angle from the particle data.
[13] R. Hemker *et al.*, *Proceedings of the 1999 Particle Accelerator Conference* (IEEE, Piscataway, NJ, 1999), p. 3672.
[14] M. J. Hogan *et al.*, Phys. Rev. Lett. **95**, 054802 (2005).
[15] P. Muggli *et al.*, Phys. Rev. Lett. **101**, 054801 (2008).
[16] S. Wilks *et al.*, IEEE Trans. Plasma Sci. **15**, 210 (1987).